Carotenoid Singlet Levels Newly Identified by Fluorescence and Fluorescence-Excitation Spectroscopy of β-Apo-8′-carotenal at 160 K

Yousuke Miki, Tadayuki Kameyama, Yasushi Koyama,* and Yasutaka Watanabe

Faculty of Science, Kwansei Gakuin University, Uegahara, Nishinomiya 662, Japan

Received: January 4, 1993; In Final Form: February 22, 1993

Fluorescence and fluorescence-excitation spectroscopy at 160 K of *all-trans*-β-apo-8′-carotenal in *n*-hexane and CS_2 solutions has identified two new singlet levels in addition to the well-documented levels of "$2^1A_g^-$" (level I), "$^1B_u^+$" (level IV), and "$^1A_g^+$" (*cis*-peak); one (level III) in between the "$2^1A_g^-$" and "$^1B_u^+$" levels and the other (level V) in between the "$^1B_u^+$" and "$^1A_g^+$" levels. The fluorescence data suggest the presence of two additional different kinds of levels, i.e., one immediately above the "$2^1A_g^-$" level (levels II and II′) and the other overlapped with the "$^1B_u^+$" level (level IV′). Two different processes of internal conversion have been found spectroscopically; one from level IV to level I and the other from level V to level III.

Introduction

In order to reveal the mechanism of the light-harvesting function of carotenoids in photosynthetic systems, the electronic energy levels of carotenoids are of primary importance.[1] In the case of a symmetric nonpolar carotenoid, extrapolation of the results of Pariser–Parr–Pople (PPP) calculations including multireference double-excitation configurational interactions (MRD-CI) for model polyenes with the number of the conjugated double bonds (*n*) up to 8 has predicted the presence of (1) the "$3^1A_g^-$" state in between the "$^1A_g^+$" and the "$^1B_u^+$" states and (2) the "$^1B_u^-$" state in between the "$^1B_u^+$" and "$2^1A_g^-$" states[2] in addition to the well-known "$^1A_g^+$" (*cis*-peak), "$^1B_u^+$" (strongly optically allowed), and "$2^1A_g^-$" (optically forbidden) states. (Hereafter this type of notation will be used with a pair of quotation marks, although the notation refers to a carotenoid having the center of symmetry).

Recent development of fluorescence spectroscopy has enabled us to identify the "$^1B_u^+$" and "$2^1A_g^-$" fluorescence levels of carotenoids: (a) Fluorescence from the "$^1B_u^+$" level has a quantum yield on the order of 10^{-5}, indicating that its lifetime is on the order of 100 fs.[3,4] (b) Fluorescence from the "$2^1A_g^-$" level peaked around 13 300 cm^{-1} was first detected for fucoxanthin in CS_2, and its 0 → 0 vibrational level was estimated to be around 15 900 cm^{-1}.[5] (c) The origin of predominant fluorescence, either the "$^1B_u^+$" state or the "$2^1A_g^-$" state, depends on the structure of the carotenoid; fluorescence from the "$^1B_u^+$" state alone was seen for neoxanthin and β-carotene (nonpolar carotenoids), fluorescence from the "$2^1A_g^-$" state alone was seen for fucoxanthin, siphonaxanthin, and peridinin (polar allenic carotenoids with a carbonyl group at one end), and fluorescence from both states was seen for β-apo-8′-carotenal.[6,7] (d) The relative intensities of fluorescence from the "$^1B_u^+$" and "$2^1A_g^-$" states changed depending on the polarizability of the solvent. The solvent effect was explained in terms of the rate of internal conversion which is proportional to the exponential of the "$^1B_u^+$"–"$2^1A_g^-$" energy gap.[8] (e) Fluorescence spectroscopy of β-carotene homologs showed that the fluorescing state depended on the number of conjugated double bonds (*n*); fluorescence from the "$2^1A_g^-$" state dominated for $n = 5$ and 7, while fluorescence from the "$^1B_u^+$" state dominated for $n = 9$ and 11 (β-carotene). The energy of the "$2^1A_g^-$" level of β-carotene ($n = 11$) was extrapolated from the energies of minicarotenes to be 14 500 ± 100 cm^{-1}.[9] (f) Fluorescence from a series of spheroidene homologs with $n = 10$ down to 7 exhibited a systematic crossover from "$^1B_u^+$" to "$2^1A_g^-$" fluorescence with decreasing chain length. The energy of the "$2^1A_g^-$" level of spheroidene ($n = 10$) could be extrapolated from the energies of the shorter homologs to be around 13 000 cm^{-1}.[10] Thus, fluorescence from the "$^1B_u^+$" and "$2^1A_g^-$" levels has now been well documented, but the exact energy of the "$2^1A_g^-$" state has not been established for ordinary carotenoids with $n = 10$ or larger.

In the present investigation, we have addressed the following two questions based on the above theoretical and experimental results so far obtained: (1) Are there additional low-lying electronic energy levels of carotenoids other than the "$2^1A_g^-$", "$^1B_u^+$", and "$^1A_g^+$" states? (2) Where is the 0 → 0 vibrational level of the "$2^1A_g^-$" state?

In order to answer these questions, the following points have been taken into consideration: (i) We have chosen β-apo-8′-carotenal because fluorescence from both the "$^1B_u^+$" and "$2^1A_g^-$" states has been detected for this carotenoid.[7,8] Further, its polar asymmetric structure may enable us to detect "optically forbidden" states together with the (n,π^*) state. (ii) In order to identify the 0–0 vibrational origin of an electronic (absorptive or fluorescent) energy level, it is crucial that the energy level is identified with a vibrational progression having an equal and acceptable spacing for a carbon–carbon stretching vibration (1600–1000 cm^{-1}). For this purpose, we have built a setup for detecting fluorescence with high sensitivity; the resultant high signal to noise (S/N) ratio enabled us to identify each vibrational structure simply by expanding the ordinate scale. (iii) We cooled down the *n*-hexane and CS_2 solutions of this carotenoid very carefully and optimized the temperature to detect the vibrational structures most clearly. (iv) We systematically changed the excitation and detection wavelengths in the region 400–1100 nm and extracted the electronic levels from a substantial amount of fluorescence and fluorescence-excitation data.

Experimental Section

Setup for Fluorescence, Fluorescence-Excitation, and Absorption Measurements. Figure 1a shows a block diagram of our homemade setup for fluorescence and fluorescence-excitation measurements. A 500-W short arc Xe lamp (Ushio UXL500D) combined with a filter (Toshiba L39 or UV35) and a monochromator (Jasco CT25ND), which was equipped with a grating of 1200 lines/mm (500 nm blaze) and slits of 2 (entrance), 3 (intermediate), and 2 (exit) mm, was used as a variable-wavelength light source for exciting emission in the 400–700-nm region. An Ar^+ laser (NEC GLG 2032) operating at 488 nm was also used as a light source for exciting emission in the 700–1200-nm region. Each sample solution which was sealed into a quartz tube (2 mm i.d. × 45 mm) was mounted in a cryostat, and its temperature was controlled in the range 10–300 K by the use of a closed-cycle

* Author to whom correspondence should be addressed.

0022-3654/93/2097-6142$04.00/0

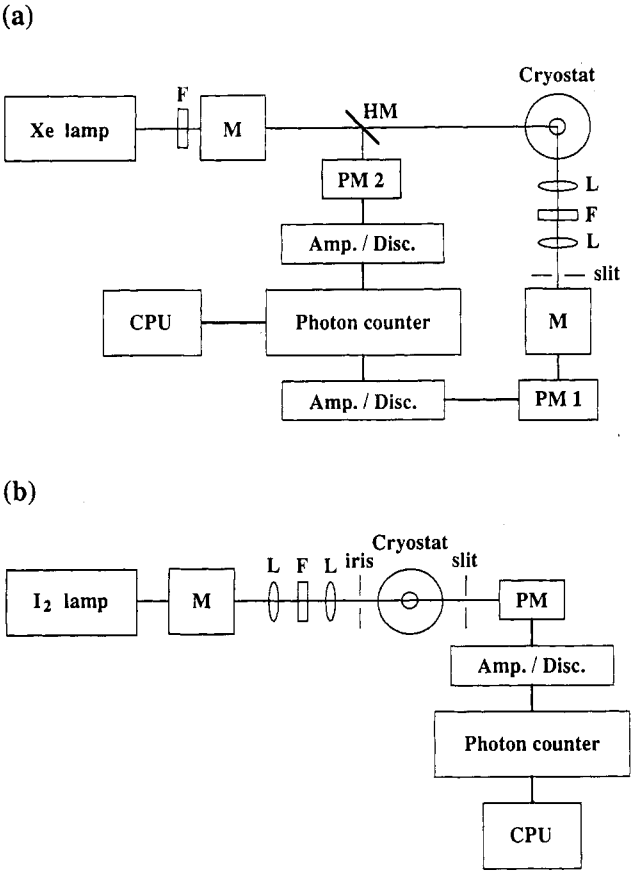

Figure 1. Block diagrams of our setups for (a) fluorescence and fluorescence-excitation and (b) absorption measurements. Abbreviations: F, filter; M, monochromator; HM, half mirror; L, lens; PM, photomultiplier; Amp., amplifier, Disc., discriminator; and CPU, central processing unit. See the Experimental Section for the details.

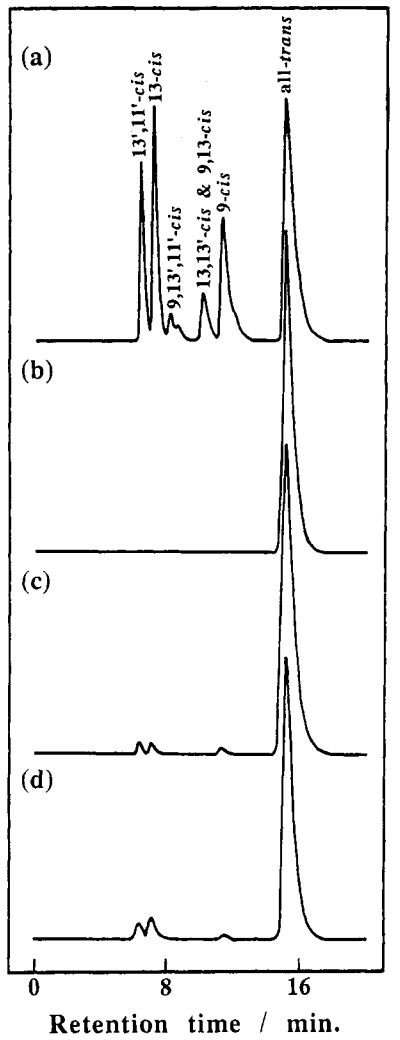

Figure 2. HPLC elution profiles of isomeric β-apo-8′-carotenal. (a) A mixture of isomers obtained by iodine-catalyzed photoisomerization, (b) *all-trans*-β-apo-8′-carotenal purified by recrystallization, (c) the sample immediately after sealing, and (d) the sample after all the fluorescence and fluorescence-excitation measurements.

helium refrigerator (Leybold-Heraeus ROK 10–300). A 90° emission was collected directly or through a standard glass filter (Toshiba R69) and then focused into a monochromator (Jasco CT25ND, which was equipped with a grating of 600 lines/mm (750 nm blaze) and slits of 1.5 (entrance), 3 (intermediate), and 1.5 (exit) mm; the output emission was detected by a GaAs photocathode detector (Hamamatsu R943–02), which is denoted as "PM1". The power of excitation was monitored by a liquid-nitrogen-cooled S1 photomultiplier (Hamamatsu R632), "PM2". The output signals of PM1 and PM2 were put into each set of amplifier and discriminator and then into a photon counter (PARC 1109). Here, the emission was recorded in a mode to compensate the fluctuation of the light source; the gate of PM1 was opened while a certain amount of photons were accumulated through PM2. The fluorescence and fluorescence-excitation data were corrected by the instrumental function which had been determined by using a standard lamp. Smoothing of the spectra was performed by averaging data for 5 data points (extending 2 data points on each side of a particular point; interval, 0.5 or 1.0 nm).

A typical input power for excitation at 500 nm, for example, was 39 μW (9.8×10^{13} photons·s^{-1}), and the photon density at the sample (spot diameter, 1.37 mm) was 2.66 mW·cm^{-2} (6.7×10^{15} photons·s^{-1}·cm^{-2}). The quantum yield of fluorescence was determined relative to Rhodamine B to be 2×10^{-5} for 498-nm excitation.

Figure 1b shows a block diagram of our setup for absorption measurements. A 300-W I_2 lamp (Ushio JC24V) combined with a monochromator (Jasco CT25ND), which was equipped with a grating of 1200 lines/mm and slits of 0.5 (entrance), 1.0 (intermediate), and 0.5 (exit) mm, was used as a light source; the beam was passed through a filter (Toshiba UV35) before irradiation of the sample. The sample was cooled by a cooling unit (Oxford DN704). The beam after passing through the sample was detected by a liquid-nitrogen-cooled photomultiplier (Hamamatsu R632).

Purity of the Sample. *All-trans*-β-apo-8′-carotenal (abbreviated as β-apo-8′-carotenal) was purchased from Fluka and recrystallized twice from *n*-hexane. A 5×10^{-5} M solution in *n*-hexane (Dojin Chemical Co., "Luminasol" or CS_2 (Cica-Merck, spectral grade) was used for spectral measurements. Figure 2 compares the HPLC elution profiles of (a) a mixture of isomers obtained by iodine-catalyzed photoisomerization, (b) *all-trans*-β-apo-8′-carotenal purified by the recrystallization, (c) the sample (*all-trans*-β-apo-8′-carotenal) immediately after sealing, and (d) the sample after all the fluorescence and fluorescence-excitation measurements. HPLC conditions were as follows: column, a 4 mm i.d. × 250 mm column packed with LiChrosorb Si-60 5 μm; eluent, 7% diethyl ether in *n*-hexane; flow rate, 1.5 mL/min; and detection, 450 nm. Each isomer was identified by ^{1}H-NMR spectroscopy (Y. Miki, H. Hashimoto, and Y. Koyama, unpublished results). The relative ε values of the *cis* isomer (when the ε value of the *all-trans* isomer at the detection wavelength is normalized to 1.0) were determined as follows: 13′,11′-*cis*, 0.773; 13-*cis*, 0.766; and 9-*cis*, 0.943. Then, the ratio of 13′,11′-*cis*:13-*cis*:9-*cis*:*all-trans* was determined to be 1.4:1.3:0.9:96.4, immediately after sealing, and 2.9:4.6:0.7:91.8, after the completion of all the measurements. Thus, the change in the composition of the isomers during the measurements was 13′,11′-*cis* (+1.5%), 13-*cis* (+3.3%), 9-*cis* (−0.2%), and *all-trans*

(-4.6 %). We recorded the fluorescence (excitation at 406 and 468 nm) and fluorescence-excitation (detection at 605 nm) spectra of the 13′,11′-*cis*, 13-*cis*, and 9-*cis* isomers; all the spectra were different from that of the *all-trans* isomer. Thus, the possibility of any contribution of the above isomers in the set of fluorescence and fluorescence-excitation spectra of the *all-trans* isomer, which will be shown in the results section, is excluded.

The absorption spectra (in the 200–600-nm region) of the set of *cis–trans* isomers after prolonged irradiation at room temperature to reach the same photostationary state were identical within the limit of experimental error, and the total amount of the carotenoid was conserved. Analysis by HPLC for the detection wavelengths in the region of 270–498 nm (10 different wavelengths) of the above mixture as well as of the *all-trans* isomer irradiated for 24 h under the experimental conditions showed only the peaks to be ascribed to the above set of isomers; no additional peaks to be ascribed to any impurity were detected. Further, a pair of fluorescence spectra, i.e., one recorded at the beginning and the other after all the fluorescence and fluorescence-excitation measurements, were the same. Thus, the possibility of any contribution of the photodegradation products in the set of fluorescence and fluorescence-excitation spectra, shown below, is excluded.

Results

Fluorescence and Fluorescence-Excitation Spectra and Energy Diagram in *n*-Hexane. Figure 3 shows a set of fluorescence (a–i) and fluorescence-excitation (j–p) spectra of *all-trans*-β-apo-8′-carotenal in *n*-hexane solution at 160 K. The absorption spectrum is shown with circles. The wavelength of each excitation or detection is shown beside each fluorescence or fluorescence-excitation spectrum; the energies of excitation and detection are shown on a scale at the bottom. Figure 4 shows an energy diagram deduced from the data in Figure 3.

In order to practically remove the contribution of the Raman lines of both the sample and the solvent in the fluorescence spectra, the input power for excitation was reduced as much as possible. Further, only the peaks which appear in the same spectral region for at least two different wavelengths of excitation were regarded as fluorescence peaks.

In the following assignments, the electronic energy levels will be numbered from the lower to the higher energies as levels I, II, III, IV, and V, and their fluorescence and absorption (fluorescence-excitation) levels will be labeled "E" (emission) and "A" (absorption), respectively. The vibrational transitions will be denoted as (0 → 0), (0 → 1), (0 → 2), ... for fluorescence and as (0 ← 0), (1 ← 0), (2 ← 0), ... for absorption. Thus, AIV(1 ← 0) stands for the absorptive transition from the vibrational level 0 of the ground state to the vibrational level 1 of level IV, while EIV(0 → 1) stands for the fluorescent transition from the vibrational level 0 of level IV to the vibrational level 1 of the ground state. In the case of the present carotenoid, it has turned out that the "$2^1A_g^-$" and "$^1B_u^+$" levels correspond to level I and level IV in our notation. Assignment of each level is described below according to the sequence of assignments:

(1) Level IV (the "$^1B_u^+$" Level) and Level IV′. The absorption spectrum shows the transition (from the ground state) to the "$^1B_u^+$" state with vibrational progresssions at 498, 468, and 442 nm, which we call the AIV(0 ← 0), AIV(1 ← 0), and AIV(2 ← 0) transitions. The set of emission spectra (Figure 3) of excitation at (a) 498, (b) 488, (c) 480, and (d) 468 nm [on and around the AIV(0 ← 0) and AIV(1 ← 0) transitions] give rise to different spectral patterns in the region of 500–560 nm where fluorescence from level IV is expected to appear, a fact which indicates that at least one additional level (level IV′) is overlapped with level IV. We assign a pair of peaks around 512 and 552 nm (averages of the observed values) to the EIV(0 → 0) and EIV(0 → 1) transitions (difference 1400 cm^{-1}), while we assign a pair of peaks

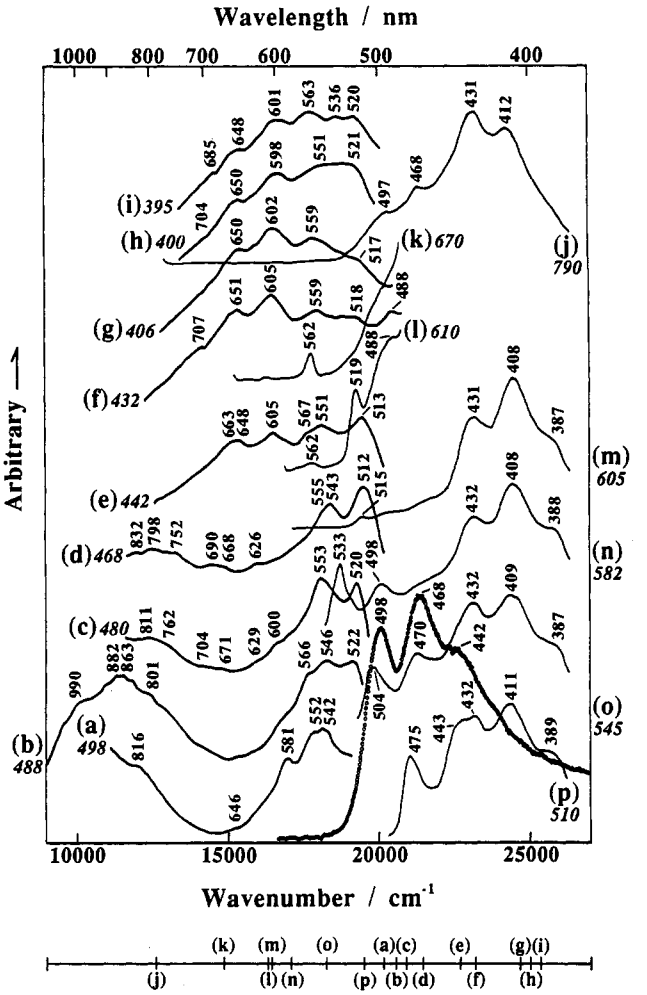

Figure 3. Absorption, emission, and fluorescence-excitation spectra of β-apo-8′-carotenal in *n*-hexane at 160 K. The absorption spectrum is shown with circles. Fluorescence spectra (thicker lines, a–i) were excited at (a) 498, (b) 488, (c) 480, (d) 468, (e) 442, (f) 432, (g) 406, (h) 400, and (i) 395 nm. Fluorescence-excitation spectra (thinner lines, j–p) were detected at (j) 790, (k) 670, (l) 610, (m) 605, (n) 582, (o) 545, and (p) 510 nm. The energy of each excitation or detection is shown on a scale at the bottom.

around 521 and 566 nm to the EIV′(0 → 0) and EIV′(0 → 1) transitions (difference 1500 cm^{-1}). The fluorescence-excitation (hereafter simply denoted as excitation) spectra at 545 and 510 nm give rise to peaks at 504 and 475 nm (not assignable to the AIV(0 ← 0) and AIV(1 ← 0) transitions), supporting the idea of overlapping level IV′. We assign the peaks in the fluorescence spectra at 497–498, 468–470, and 443 nm to the AIV(0 ← 0), AIV(1 ← 0), and AIV(2 ← 0) absorptions (these correspond to the above absorption peaks at 498, 468, and 442 nm) and the above peaks at 504 and 475 nm to the AIV′(0 ← 0) and AIV′(1 ← 0) absorptions.

(2) Level I (the "$2^1A_g^-$" Level) and Level II(II′). Emission spectra of 498- and 480-nm excitation indicate the presence of a peak above 800 nm, and the emission spectrum at 488-nm excitation shows a series of peaks at 801, 882, and 990 nm, which we assign to the EI(0 → 0), EI(0 → 1), and EI(0 → 2) transitions. This electronic level is regarded as the "$2^1A_g^-$" level.[7] The excitation spectrum detected at 790 nm shows the AIV(0 ← 0) and AIV(1 ← 0) absorptions at 497 and 468 nm which correspond to the 498 and 468 absorptions in the absorption spectrum and prove that the EI fluorescence originates from the particular carotenoid.

The emission spectrum of 468-nm excitation shows a pair of progressions, i.e., one at 626 and 690 nm and the other at 668 and 752 nm; the former progression is assigned to the EII(0 → 0) and EII(0 → 1) transitions, and the latter progression is assigned

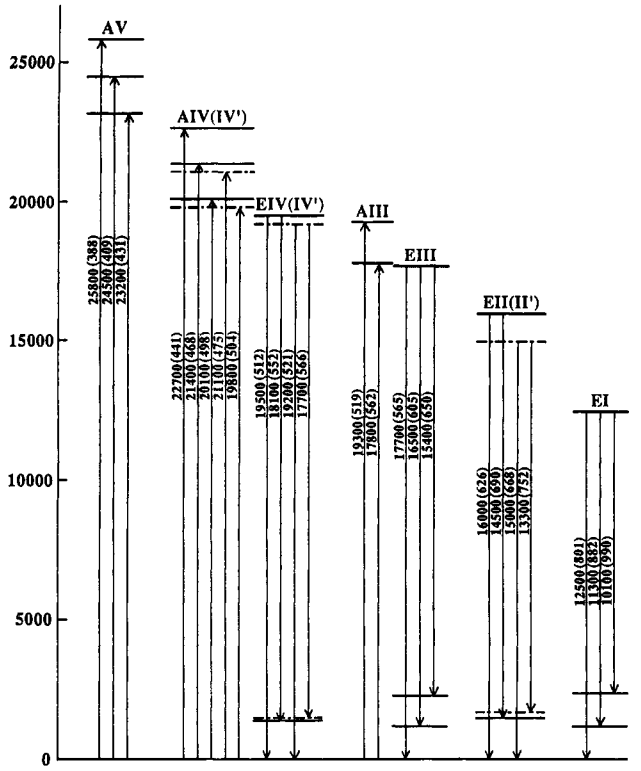

Figure 4. An energy diagram of β-apo-8′-carotenal in *n*-hexane which is deduced from the data in Figure 3.

to the EII′(0 → 0) and EII′(0 → 1) transitions. Additional experiments are necessary to establish these weak emissions.

(3) Level III and Level V. Emission spectra at 442-, 432-, 406-, 400-, and 395-nm excitations show peaks around 605 and 650 nm, in addition to the peaks in the 510–570-nm region which were ascribed above to the EIV and EIV′ transitions. We ascribe the 605- and 650-nm peaks to fluorescence from a new level, which we call level III; they are assigned to the EIII(0 → 1) and EIII(0 → 2) transitions. The peaks are most strongly enhanced at 432- and 406-nm excitation. (These wavelengths corresponds to the AV(0 ← 0) and AV(1 ← 0) transitions, *vide infra*.) The EIII(0 → 0) transition was determined to be 565 nm by using the difference of spectrum f, Figure 3, (highest EIII contribution) minus spectrum d, Figure 3, (negligible EIII contribution). Peaks at 562 and 519 nm in the excitation spectra of 670- and 610-nm detection are assigned to the AIII(0 ← 0) and AIII(1 ← 0) transitions.

All the excitation spectra, which were detected in the entire region of the EI, EII(EII′), EIII, and EIV fluorescence (more specifically, detection at 790, 605, 582, 545, and 510 nm), show three peaks around 431, 409, and 388 nm. We ascribe them to an absorptive electronic transition of a new level, which we call level V; they are assigned to the AV(0 ← 0), AV(1 ← 0), and AV(2 ← 0) transitions. These absorptions are much lower in energy than the absorption band of the "$^1A_g^+$" state called "*cis*-peak"; the latter appears clearly at 330 nm in the case of the 13-*cis* isomer.

These two electronic levels, i.e., level III and level V, have been identified for the first time. The possibility that the EIII fluorescence and AV absorption originate from any impurity other than *all-trans*-β-apo-8′-carotenal may be excluded by the following argument: Fluorescence from the "$^1B_u^+$" level (level IV in the present carotenoid) and that from the "$2^1A_g^-$" level (level I) have been well documented for a variety of carotenoids (see the Introduction section). There remains little doubt in the EI and EIV fluorescence. (1) The excitation spectra detected at the wavelengths of these fluorescences give rise to the peaks assigned to level V (in addition to the absorption peaks assigned to level IV). Thus, the excitation peaks of level V should be ascribed to

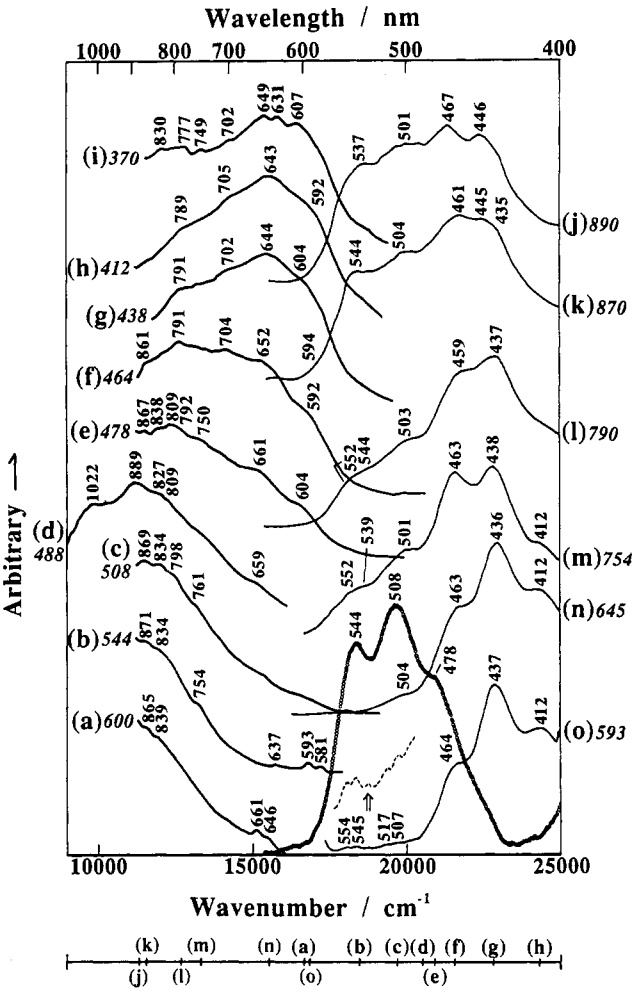

Figure 5. Absorption, emission, and fluorescence-excitation spectra of β-apo-8′-carotenal in CS_2 at 160 K. The absorption spectrum is shown with circles. Fluorescence spectra (thicker lines, a–i) were excited at (a) 600, (b) 544, (c) 508, (d) 488, (e) 478, (f) 464, (g) 438, (h) 412, and (i) 370 nm. Fluorescence-excitation spectra (thinner lines, j–o) were detected at (j) 890, (k) 870, (l) 790, (m) 754, (n) 645, and (o) 593 nm. The energy of each excitation or detection is shown on a scale at the bottom (except for spectrum i, 370 nm).

the particular carotenoid. (2) Excitation at the wavelength of level V gives rise to fluorescence peaks assigned to level III (in addition to fluorescence peaks assigned levels IV and IV′), level III then should be ascribed to this carotenoid. (3) The carotenoid does exhibit a very peculiar fluorescence pattern, which is characterized by "a pair of extremely large Stokes shifts"; in other words, fluorescence from level I takes place when level IV is excited, while fluorescence from level III takes place when level V is excited. This must be a characteristic intrinsic to this particular carotenoid. Actually, no indication of impurity or isomers has been found experimentally; see the Experimental Section.

Fluorescence and Fluorescence-Excitation Spectra and Energy Diagram in CS_2. Figure 5 shows a set of fluorescence (a–i) and fluorescence-excitation (j–o) spectra of *all-trans*-β-apo-8′-carotenal in CS_2 at 160 K. The absorption spectrum is shown with circles. The wavelength of each excitation or detection is shown beside each fluorescence or fluorescence-excitation spectrum; the energies of excitation and detection are shown on a scale at the bottom. Figure 6 shows an energy diagram deduced from the data in Figure 5.

(1) Level IV (the "$^1B_u^+$" Level) and Level IV′. The absorption spectrum shows the transition to the "$^1B_u^+$" level (level IV) with vibrational progressions at 544, 508, and 478 nm, which we assign to the AIV(0 ← 0), AIV(1 ← 0), and AIV(2 ← 0) transitions. The fluorescence spectra detected at 600- and 544-nm excitation

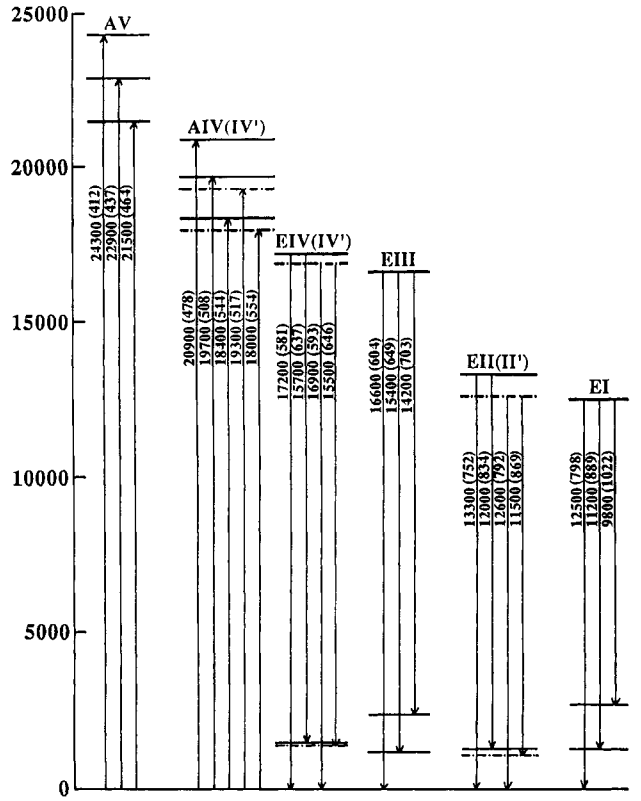

Figure 6. An energy diagram of β-apo-8'-cartenal in CS_2 which is deduced from the data in Figure 5.

show peaks at 581 and 637 nm as well as those at 593 and 646 nm, the pairs of which we ascribe to the vibrational progressions of level IV and level IV'. The excitation spectrum at 593-nm detection shows four peaks (see the blow-up shown in a dashed line in Figure 5); we assign the peaks at 545 and 507 nm to the AIV(0 ← 0) and AIV(1 ← 0) transitions (they correspond to the absorption peaks at 544 and 508 nm), while we assign the peaks at 554 and 517 nm to the AIV'(0 ← 0) and AIV'(1 ← 0) transitions.

(2) Level I (the "$2^1A_g^-$" Level) and Level II(II'). The fluorescence spectra of 600-, 544-, and 508-nm excitation indicate fluorescence from the "$2^1A_g^-$" level below 750 nm. The fluorescence spectrum at 488-nm excitation clearly shows its vibrational progression. We picked out a peak at 798 nm of 508-nm excitation and peaks at 889 and 1022 nm of 488-nm excitation (no Raman lines are expected in this region) and assigned them to the EI(0 → 0), EI(0 → 1), and EI(0 → 2) transitions, the spacings being 1300 and 1400 cm^{-1}. The fluorescence-excitation spectra detected at 870 and 790 nm show broad peaks which roughly correspond to the 544- and 508-nm absorption peaks, a fact which ensures that the EI fluorescence originates from the present carotenoid.

The peak around 752 nm (an averaged value) in the fluorescence spectra of 544-, 508-, and 478-nm excitation and the other peak around 834 nm in the fluorescence spectra of 544-, 508-, 488-, and 478-nm excitation are tentatively assigned to the EII(0 → 0) and EII(0 → 1) transitions. The peak around 792 nm in the fluorescence spectra of 478-, 464-, 438-, and 412-nm excitation and the peak around 869 nm in the fluorescence spectra of 600-, 544-, 508-, and 478-nm excitation is tentatively assigned to the EII'(0 → 0) and EII'(0 → 1) transitions. Additional experiments are necessary to establish these weak emissions.

(3) Level III and Level V. The fluorescence spectra of 464-, 438-, 412-, and 370-nm excitation show strong peaks around 649 and 703 nm, which we assign to fluorescent transitions from level III, i.e., the EIII(0 → 1) and EIII(0 → 2) transitions. A peak at 604 nm of 438- and 478-nm excitation is picked out and assigned to the EIII(0 → 0) transition.

Fluorescence-excitation spectra at 790-, 754-, 645-, and 593-nm detection show strong peaks around 464, 437, and 412 nm, which we ascribe to fluorescence from level V; they are assigned to the AV(0 ← 0), AV(1 ← 0), and AV(2 ← 0) transitions. (The fluorescence-excitation pattern is slightly changed when detected in the EI region, i.e., at 890 and 870 nm.) Fluorescence from level III is strongly enhanced when excited at the above AV vibrational transitions, i.e., at 464, 438, and 412 nm. A slightly different fluorescence pattern is obtained when excited around the "*cis*-peak" (see the spectrum of 370-nm excitation).

Solvent Effect on Energy Levels, and Solvent and Temperature Effects on Internal Conversion Pathways. The set of fluorescence and fluorescence-excitation spectra in *n*-hexane (Figure 3) show that there are two different pathways of internal conversion: The fluorescence-excitation spectra of 790- and 605-nm detection, for example, show that the fluorescence intensity upon AV excitation is much higher than that upon AIV excitation. When the carotenoid molecule is excited through the AIV electronic transition, weak fluorescence appears from the EI and EIV levels (spectra a–d, Figure 3). On the other hand, when the molecule is excited through the AV transition, strong fluorescence takes place from both the EIV and EIII levels (spectra f–i, Figure 3). The results indicate that there are two different pathways of internal conversion, i.e., one from level IV to level I and the other from level V to level III. The internal conversion process starting from level IV may dissipate most of the input energy through nonradiative transitions; the internal conversion process from level V is much more efficient and gives rise to a much higher quantum yield of fluorescence from level III.

The set of fluorescence and fluorescence-excitation spectra in CS_2 (Figure 5) also show two different pathways of internal conversion: When the molecule is excited through the AIV transition, strong fluorescence takes place from the EI level. Similarly, when the molecule is excited through the AV transition, strong fluorescence takes place from the EIII level. The fluorescence-excitation spectra of 890- and 645-nm detection show that the efficiencies of internal conversion pathways, i.e., one from level IV to level I and the other from level V to level III, have comparative orders of magnitude in this solvent.

The solvent effect on the internal conversion pathways is thus summarized as follows: In *n*-hexanes, the internal conversion process from level IV to level I dissipates most of the input light energy and only small amount of energy is emitted from level I, but in CS_2, the input energy is conserved and then emitted from level I. The internal conversion from level V to level III does not exhibit such a large solvent effect.

Comparison of the energy diagrams in *n*-hexane (Figure 4) and in CS_2 (Figure 6) elucidates the solvent effect on the electronic energy levels. Replacement of the solvent, *n*-hexane, by CS_2 shifts levels V, IV, III, II, and I to the lower energies by 1600, 1700, 1100, 2700, and ~0 cm^{-1}; the shifts of levels IV' and II' are similar to those of levels IV and II, respectively. Level I exhibits a negligible solvent effect, supporting its assignment to the "$2^1A_g^-$" state. Less efficient (more efficient) intramolecular energy transfer from level IV to level I in *n*-hexane (CS_2) is explained in terms of the larger (smaller) energy gap between level IV and level I, i.e., 7000 cm^{-1} (4700 cm^{-1}). Most probably, level III is not involved in the energy transfer from level IV to level I, but level II(II'), which shows the largest solvent effect of 2700 cm^{-1}, may be involved in this energy transfer.

Figure 7 shows the temperature dependence, from 120 K up to room temperature, of fluorescence from level III in (a) *n*-hexane and (b) CS_2 solutions. The EIII fluorescence in *n*-hexane solution (excitation at 432 nm) is negligible below 120 K, it reaches a maximum around 160 K, and it becomes weaker again at higher temperatures. This strange behavior may be explained in terms of a pair of barriers to enter and to leave the potential surface of level III. Based on the temperature dependence in the 120–

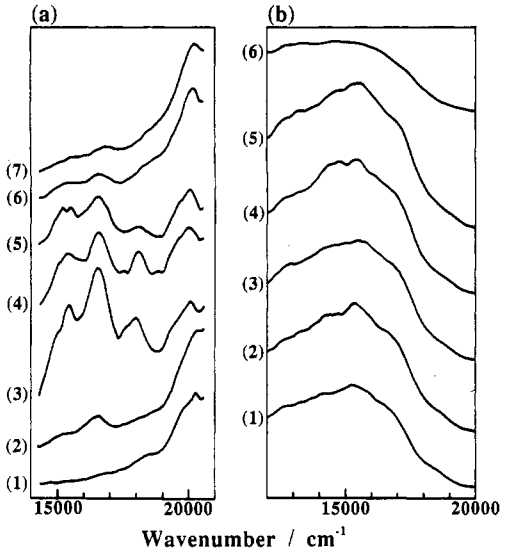

Figure 7. Temperature dependence of emission from level III. (a) *n*-Hexane solution (432-nm excitation) at (1) 120, (2) 140, (3) 160, (4) 180, (5) 200, (6) 250 and (7) 298 K. (b) CS_2 solution (438-nm exciation) at (1) 120, (2) 140, (3) 160, (4) 170, (5) 190 and (6) 298 K.

160 K region, the barrier height of the internal conversion from level V to level III was determined to be 887 cm^{-1}. The EIII fluorescence persists even at room temperature.

The EIII fluorescence in CS_2 solution (excitation at 438 nm) gradually increases from the lowest to the highest temperatures; it reaches to a maximum in the 170–190 K region, and it becomes weaker toward room temperature. The temperature-dependent variation of the fluorescence intensity is much smaller in this solution, and the fluorescence is still very strong at room temperature.

Discussion

Electronic Energy Levels Newly Identified in the Present Investigation. As the answer to the first question addressed in the Introduction, we have identified, for the first time, two electronic energy levels, i.e., one (level III) in between the "$2^1A_g^-$" and the "$^1B_u^+$" states and the other (level V) in between the "$^1B_u^+$" and "$^1A_g^+$" states. This result materializes the prediction by the PPP-MRD-CI calculations done by Tavan and Schulten.[2] Based on their results, we tentatively assign level III and level V to the "$^1B_u^-$" and the "$3^1A_g^-$" states, respectively, although no information concerning the symmetry of the energy levels has been obtained in the present investigation. The energies of the $0 \leftarrow 0$ absorptive and the $0 \rightarrow 0$ emissive transitions (hereafter, the energy values of *emissive* transitions will be given in a pair of parentheses) of the present carotenoid for the "$^1B_u^-$", "$^1B_u^+$", and "$3^1A_g^-$" states were 17 800 (17 700), 20 100 (19 500), and 23 200 cm^{-1} in *n*-hexane and (16 600), 18 400 (17 200), and 21 500 cm^{-1} in CS_2. We have determined the corresponding energy levels for spheroidene free in *n*-hexane and CS_2 solutions:[11] The energies of the "$^1B_u^-$", "$^1B_u^+$", and "$3^1A_g^-$" states were 18 700, 20 200 (20 000), and 24 100 cm^{-1} in *n*-hexane and 18 100, 18 700 (18 200), and 23 400 cm^{-1} in CS_2. The results strongly suggest that the newly found "$^1B_u^-$" (level III) and "$3^1A_g^-$" (level V) states are ubiquitous among the carotenoids, and that these levels originate from the carbon–carbon double-bond system. No energy levels corresponding to level II(II') of the present carotenoid were found in spheroidene, and therefore, the particular level(s) should be ascribed to the (n,π^*) transition of the terminal carbonyl group. The largest solvent effect of level II(II') (*vide supra*) supports this assignment, since the polarization of the carbonyl group is supposed to be sensitive to the polarizability of the solvent.

We have also identified, for the first time, an internal conversion process from the "$3^1A_g^-$" state (level V) to the "$^1B_u^-$" state (level III) in addition to the well-documented internal conversion process from the "$^1B_u^+$" state (level IV) to the "$2^1A_g^-$" state (level I).[8] The efficiency of those processes depended on the solvent and the temperature. In the case of spheroidene free in solutions, an internal conversion process took place from the "$3^1A_g^-$" state to the "$2^1A_g^-$" state, instead: When the "$3^1A_g^-$" state was excited, fluorescence from the "$2^1A_g^-$" state was enhanced; when the "$^1B_u^+$" state was excited, fluorescence took place from the "$^1B_u^+$" state itself. Therefore, the above pair of internal conversion processes seem to be inherent to the present carotenoid.

All the above results indicate that the energy levels and the internal conversion processes strongly depend on (1) the kind of carotenoids, (2) the polarizability, and (3) the temperature of the solutions.

The Energy of the "$2^1A_g^-$" Level. As the answer to the second question in the Introduction, we have determined the energy of the "$2^1A_g^-$" state of the present carotenoid to be (12 500) cm^{-1} (as the $0 \rightarrow 0$ emissive transition) in both *n*-hexane and CS_2 solutions. The energy of the "$2^1A_g^-$" state for spheroidene was 14 900 (14 900) cm^{-1} in *n*-hexane and 14 600 (14 600) cm^{-1} in CS_2. We have also determined the energy of the "$2^1A_g^-$" state for β-carotene to be 13 200 (13 100) cm^{-1} in *n*-hexane and 13 000 cm^{-1} in CS_2 (T. Kameyama, Y. Watanabe, Y. Miki, and Y. Koyama, unpublished results). The energy of the "$2^1A_g^-$" state was little affected by the kind of solvent in all the carotenoids. As for dependence on the carotenoid structure, the "$2^1A_g^-$" energy was in the order, spheroidene ($n = 10$) > β-carotene ($n = 11$) > β-apo-8'-carotenal ($n = 10$). The order is not simply a function of the number (n) of the conjugated chain. The "$2^1A_g^-$" level of the present carotenoid may be pushed downward by the additional (n,π^*) level of the terminal carbonyl group (levels II and II'), which is located just above the "$2^1A_g^-$" state (level I).

The Possibility of Fluorescence from the Breakdown Product or Aggregate of the Carotenoid. The present carotenoid showed peculiar fluorescence characteristics, and none of the fluorescence-excitation spectra clearly traced out the absorption spectrum. The result most probably derives from the following facts: (1) Fluorescence from the optically-active "$^1B_u^+$" state is extremely weak, and the carotenoid has unique and efficient internal conversion pathways, and (2) we are still unable to find experimental conditions to obtain such a fluorescence-excitation spectrum. This important point has been alluded to by one of the reviewers, and he (she) has strongly questioned our present interpretation that fluorescence peaks in the 600–700-nm region and fluorescence-excitation peaks below 460 nm originate from the carotenoid, β-apo-8'-carotenal. The reviewer claims that the above peaks must originate from some breakdown product of the carotenoid showing the following characteristics: (1) It has a shorter conjugated chain; (2) it fluoresces much more strongly than the carotenoid; (3) it also exhibits a large "Stokes shift"; and (4) it could not be detected by our HPLC technique. Strictly speaking, the above possibility cannot completely be ruled out, although we have tried to establish the purity of the sample, and presented similar but slightly different fluorescence characteristics of another carotenoid, spheroidene. Presently, we have no experimental data either to confirm or to negate the reviewer's claim. We believe that it is most important, at the present stage, to collect a large amount of data for a variety of carotenoids and to present systematic changes in both the energy levels and the internal conversion processes depending on the length of the conjugated chain and also on the terminal group. The results should establish the energy levels and the unique internal conversion processes of all the carotenoids and also should help to understand the mechanisms of the light-harvesting function as well as the implication of the natural selection of polar asymmetric carotenoids (xanthophylls) in algae and higher plants.

The reviewer also points out the following possibilities: (a) emission from the excited singlet states is competing with

vibrational relaxation and (b) aggregates of the molecules are being formed. As for the latter possibility, fluorescence data at lower concentrations should be most important, although we will have to improve the sensitivity of our setup in order to deal with more diluted solutions. The possibility that a pair of almost degenerate levels (level IV′ and level II′) are due to an aggregate cannot be excluded. Further investigations are required to fully solve the above problems.

Acknowledgment. The authors wish to thank Professor Harry A. Frank for sending the manuscript of ref 10 prior to publication. We also thank Dr. Mamoru Mimuro for sending the detailed results of spectral deconvolution described in ref 6. The authors wish to thank one of the reviewers for the criticism described above.

References and Notes

(1) Koyama, Y. *J. Photochem. Photobiol. B: Biol.* **1991**, *9*, 265.
(2) Tavan, P.; Schulten, K. *J. Chem. Phys.* **1986**, *85*, 6602.
(3) Gillbro, T.; Cogdell, R. J. *Chem. Phys. Lett.* **1989**, *158*, 312.
(4) Shreve, A. P.; Trautman, J. K.; Owens, T. G.; Albrecht, A. C. *Chem. Phys. Lett.* **1991**, *178*, 89.
(5) Katoh, T.; Nagashima, U.; Mimuro, M. *Photosynth. Res.* **1991**, *27*, 221.
(6) Mimuro, M.; Nagashima, U.; Takaichi, S.; Nishimura, Y.; Yamazaki, I.; Katoh, T. *Biochim. Biophys. Acta* **1992**, *1098*, 271.
(7) Mimuro, M.; Nishimura, Y.; Yamazaki, I.; Katoh, T.; Nagashima, U. *J. Lumin.* **1992**, *51*, 1.
(8) Mimuro, M.; Nagashima, U.; Nagaoka, S.; Nishimura, Y.; Takaichi, S.; Katoh, T.; Yamazaki, I. *Chem. Phys. Lett.* **1992**, *191*, 219.
(9) Andersson, P. O.; Gillbro, T.; Asato, A. E.; Liu, R. S. H. *J. Lumin.* **1992**, *51*, 11.
(10) DeCoster, B.; Christensen, R. L.; Gebhard, R.; Lugtenburg, J.; Farhoosh, R.; Frank, H. A. *Biochim. Biophys. Acta* **1992**, *1102*, 107.
(11) Watanabe, Y.; Kameyama, T.; Miki, Y.; Kuki, M.; Koyama, Y. *Chem. Phys. Lett.*, in press.